Humu-2014-0513

Research Article

Expanding the Mutation Spectrum affecting αIIbβ3 integrin in Glanzmann Thrombasthenia: Screening of the *ITGA2B* and *ITGB3* genes in a Large International Cohort

Alan T. Nurden[1], Xavier Pillois*[1,2], Mathieu Fiore*[2], Marie-Christine Alessi[3], Mariana Bonduel[4], Marie Dreyfus[5], Jenny Goudemand[6], Yves Gruel[7], Schéhérazade Benabdallah-Guerida[8], Véronique Latger-Cannard[9], Claude Négrier[10], Diane Nugent[11], Roseline d'Oiron[12], Margaret L. Rand[13], Pierre Sié[14], Marc Trossaert[15], Lorenzo Alberio[16], Nathalie Martins[17], Peggy Sirvain-Trukniewicz[17], Arnaud Couloux[17], Mathias Canault[3], Juan Pablo Fronthroth[4], Mathilde Fretigny[10], Paquita Nurden[1,3], Roland Heilig[17], Christine Vinciguerra[10]

[1]Institut de Rhythmologie et de Modélisation Cardiaque, Plateforme Technologique d'Innovation Biomédicale, Hôpital Xavier Arnozan, Pessac, France; [2]Université de Bordeaux, INSERM U1034, Pessac, France; [3]Laboratoire d'Hématologie, Hôpital La Timone, Marseille, France; [4]Laboratorio de Hemostasia y Thrombosis, Service de Hematologia y Oncologia, Hospital de Pediatria "Professor Juan P Garrahan", Buenos Aires, Argentina; [5]Service d'Hématologie Biologique, CHU de Bicêtre, Le Kremlin-Bicêtre, France; [6]Laboratoire d'Hématologie, Hôpital Cardiologique, Lille, France;

This article has been accepted for publication and undergone full peer review but has not been through the copyediting, typesetting, pagination and proofreading process, which may lead to differences between this version and the Version of Record. Please cite this article as doi: 10.1002/humu.22776.

[7]Service d'Hématologie-Hémostase, Hôpital Trousseau, Tours, France; [8]Laboratoire d'Hématologie, Hôpital Cheikh Zaïd, Rabat, Morocco; [9]Service d'Hématologie Biologique, Hôpital de Brabois, CHU de Nancy, Vandoeuvre-les-Nancy, France; [10]Unité d'Hémostase Clinique, Centre Régional de Traitement de l'Hémophilie, Lyon, France; [11]Division of Hematology, Children's Hospital of Orange County, Orange, CA, USA; [12]Centre de Traitement de l'Hémophilie et des Maladies Hémorragiques Constitutionnelles, CHU de Bicêtre, Le Kremlin-Bicêtre, France; [13]Division of Haematology/Oncology, The Hospital for Sick Children, Toronto, Canada; [14]Laboratoire d'Hématologie, Hôpital Purpan, CHU Toulouse, Toulouse, France; [15]Laboratoire d'Hématologie, CHU de Nantes, Hôpital Hôtel-Dieu, Nantes, France; [16]Service et Laboratoire Central d'Hématologie, Central Hospitalier Universitaire Vaudois, Lausanne, Switzerland; [17]CEA - Institut de Génomique, Genoscope, Centre National de Séquencage, Université d'Evry and Unité Mixte de Recherche N°8030, CNRS, Evry, France

*These authors contributed equally to the study.

Correspondence: Alan T. Nurden: PTIB-LIRYC, Hôpital Xavier Arnozan, 33600 Pessac, France. Tel: 33.5.57.10.28.51; Fax 33.5.57.10.28.64; e-mail: nurdenat@gmail.com

Contract grant sponsors: This study was financed by contract N° AP07/08.42 with the Génoscope d'Evry and from INSERM (ANR-08-GENO-028-03).

Abstract

We report the largest international study on Glanzmann thrombasthenia (GT), an inherited bleeding disorder where defects of the *ITGA2B* and *ITGB3* genes cause quantitative or qualitative defects of the αIIbβ3 integrin, a key mediator of platelet aggregation. Sequencing of the coding regions and splice sites of both genes in members of 76 affected families identified 78 genetic variants (55 novel) suspected to cause GT. Four large deletions or duplications were found by quantitative real-time PCR. Families with mutations in either gene were indistinguishable in terms of bleeding severity that varied even among siblings. Families were grouped into type I and the rarer type II or variant forms with residual αIIbβ3 expression. Variant forms helped identify genes encoding proteins mediating integrin activation. Splicing defects and stop codons were common for both *ITGA2B* and *ITGB3* and essentially led to a reduced or absent αIIbβ3 expression; included was a heterozygous c.1440-13_c.1440-1del in intron 14 of *ITGA2B* causing exon skipping in 7 unrelated families. Molecular modeling revealed how many missense mutations induced subtle changes in αIIb and β3 domain structure across both subunits thereby interfering with integrin maturation and/or function. Our study extends knowledge of Glanzmann thrombasthenia and the pathophysiology of an integrin.

Keywords: Glanzmann thrombasthenia; *ITGA2B*; *ITGB3*; integrin αIIbβ3; molecular modeling

Introduction

Glanzmann thrombasthenia (GT; MIM# 273800) is an inherited rare bleeding syndrome caused by an absence of platelet aggregation. Although platelets recruit to sites of vessel injury, they fail to spread or form the platelet-to-platelet bonds essential for thrombus build up [George et al., 1990; Coller and Shattil, 2008; Nurden et al., 2011]. The molecular basis of GT is an absence or severe deficiency of the αIIbβ3 integrin (formerly designated the GPIIb-IIIa complex). Rare variant forms are given by qualitative defects of normally or partially expressed integrin while low platelet numbers and increases in platelet size are occasionally seen [Nurden et al., 2011; 2013]. Clot retraction and endocytosis of platelet-bound fibrinogen (Fg) to α-granules are frequently defective but can be retained in patients with residual αIIbβ3. While aggregation is mediated by activation-dependent binding of Fg to αIIbβ3, another mechanism and different amino acids are responsible for platelet attachment to fibrin [Podolnikova et al., 2014].

The *ITGA2B* (MIM# 607759) and *ITGB3* (MIM# 173470) genes closely localize on chromosome 17 and code for αIIbβ3 [Wilhide et al., 1997]. Although αIIb is mainly exclusive to the megakaryocyte (MK) lineage, β3 is widely distributed in tissues associated with αv as the vitronectin receptor. Transcripts for αIIb and β3 are present early in MK development with αIIb synthesized as a pro-peptide [Mitchell et al., 2006]. Ca^{2+}-dependent complex formation between pro-αIIb and β3 is a key early step; the integrin then undergoes a series of O- and N-glycosylations and posttranslational modifications in the endoplasmic reticulum (ER) and the Golgi apparatus. The mature subunits have single transmembrane domains and short cytoplasmic tails that have a salt-link between β3D723 and αIIbR995 as well as interactions with cytoskeletal and cytoplasmic proteins including talin and kindlin-3

[Yang et al., 2009]. Like other integrins, αIIbβ3 can mediate bidirectional signaling [Shattil and Newman, 2004; Coller and Shattil, 2008].

Major structural extracellular features of αIIb include the N-terminal β-propeller followed by the thigh, calf-1 and calf-2 domains; whereas for β3 the N-terminal PSI (plexin/semaphorin/integrin) domain is followed by hybrid, βI (βA), disulfide-rich EGF (epidermal growth factor) and membrane proximal β-tail domains [Xiao et al., 2004; Eng et al., 2011]. βI domain contains the functionally important MIDAS (metal ion-dependent adhesion site), ADMIDAS (adjacent to MIDAS) and SYMBS (synergistic metal binding site). Crystallography showed resting αIIbβ3 in a bent structure that straightens on platelet activation in parallel with exposure of determinants that bind Fg and other adhesive ligands to the headpiece [Zhu et al., 2013]. Nevertheless, the classical concept of a bent "non-activated" integrin has recently been challenged [Choi et al., 2013].

GT is caused by nonsyndromic genetic variants across both *ITGA2B* (30 exons) and *ITGB3* (15 exons) (D'Andrea et al., 2002; Peretz et al., 2006; Kannan et al., 2009; Jallu et al., 2010; Nurden et al., 2011; 2013). Approximately 200 mutations are currently found on the GT database (http://sinaicentral.mssm.edu/intranet/research/glanzmann/menu). Mutations include splice defects and stop codons that interfere with or abrogate mRNA synthesis while small deletions (del) and insertions (ins) with frameshifts are common. Large gene deletions are rare [Burk et al., 1991; Djaffar et al., 1993; Rosenberg et al., 1997]. Mostly, they affect αIIbβ3 synthesis or maturation; however missense mutations allowing partial or normal αIIbβ3 expression have helped identify functional domains [Loftus et al., 1990; Bajt et al., 1992; Chen et al., 1992]. Although mutations affecting β3 are predicted to extend to other tissues, mucocutaneous bleeding is the predominant characteristic of GT [George et al., 1990; Seligsohn, 2012].

We now report gene screening for 76 families with GT in much the largest study to be reported; results were compared to phenotype and bleeding severity. Sanger sequencing identified 78 potentially pathological mutations (55 novel) spread across both genes while quantitative PCR identified 4 large deletions or duplications. In silico modeling enabled an assessment of the effects of novel amino acid substitutions on αIIbβ3 structure. This international study considerably extends current knowledge of the molecular basis of GT.

Patients, Material and Methods

Patient selection

Genotyping was initially offered to GT patients in France under the terms of a contract (N°132/AP 2007-2008) between the French National Platelet Reference Center (Dr. P. Nurden, Bordeaux) and the Genomics Institute of the Commissariat à l'Energie Atomique (Professor J Weissenbach, Genoscope, Evry). This involved sequencing the *ITGA2B* genes and the *ITGB3* genes for 90 patients. The study was subsequently opened on a random international basis (Argentina, Canada, Morocco, Spain, Switzerland, USA) until the 90 patients were obtained. In the final analysis we include 76 families representing 83 cases. From the original 90 patients, two were withdrawn when the original diagnosis of GT was not confirmed while for 5 patients the isolated DNA either failed quality control or the patients were unavailable for necessary follow-up studies. Written informed consent was obtained for DNA sequencing according to the laws of the country and the study performed under the promotion of the Ethics Committee of the French National Institute of Health and Medical Research (INSERM: RBM 01-14). Patient inclusion was based on a history of mucocutaneous bleeding: major symptoms include epistaxis, easy bruising, hematomas, ecchymoses, petechiae, gingivorrhagia, heavy bleeding at menarche and menometrorrhagia,

post-partum hemorrhage, gastrointestinal (GI) bleeding, post-invasive bleeding; all symptoms typical of GT [George et al., 1990; Seligsohn, 2012]. Also required was an absent or a severely decreased platelet aggregation with at least 3 agonists (e.g. ADP, collagen and thrombin receptor activating peptide (TRAP)) and a normal or cyclical GPIb-dependent ristocetin-induced platelet agglutination. An absent or severely reduced platelet expression of αIIbβ3 in flow cytometry and/or after detection of the two subunits by Western blotting (WB) using SDS-soluble platelet extracts allowed definition of the type I (<5% αIIbβ3) and type II subgroups (5-25% αIIbβ3) [George et al., 1990]. In the case of qualitative defects of αIIbβ3, the requirement was an inability of ADP to induce the binding of Fg or PAC-1 (Becton Dickinson, New Jersey, USA) to platelets; PAC-1 recognizes an activation determinant close to the Fg-binding site. All platelet function tests were performed locally using the standard procedures of each Centre. A questionnaire was completed for each patient and included information on the patient's age and sex, country of origin, consanguinity, history of the disease, whether other family members were affected (and if genetic testing had been performed), nature and frequency of bleeding, treatment and the presence or not of anti-αIIbβ3 platelet antibodies (produced after transfusion or pregnancy when the patient's immune system comes into contact with normal platelets). A summary of the clinical and biological data obtained for each patient is provided in Supp. Table S1. A World Health Organization (WHO) bleeding score was established retrospectively for each patient: Grade 0, no bleeding; 1, mild petechial or minimal bleeding; 2, occasional significant bleeding requiring transfusion or recombinant FVIIa; 3, repeated episodes of bleeding requiring multiple transfusions or other treatments; 4, major or life threatening bleeding and hospitalizations [Bercovitz and O'Brien, 2012]. Data was assessed for statistical significance in selected groups using the two-sided Fisher's Exact Test.

DNA sequencing

EDTA-anticoagulated whole blood or the leukocyte-rich buffy coat was used for DNA extraction in each Centre or using the QIamp DNA Blood Mini kit (Qiagen, Courtaboeuf, France) after being sent to Bordeaux or Lyon. Coded samples were sent to the Genoscope for sequencing (National DNA Sequencing Centre, Evry, France). Included were two patients (GT9 and GT10) for whom single heterozygous mutations had previously been detected by Sanger sequencing following single strand conformation polymorphism analysis (SSCP) [see Peyruchaud et al., 1998; Nurden et al., 2002] and for whom a second non-detected heterozygous mutation was presumed. Technical details of our screening strategy and primer design, PCR conditions, sequencing analysis, the in silico analysis of genetic variants are to be found in Supp. Methods. Sanger sequencing ensured coverage of exons and splice sites of the *ITGA2B* and *ITGB3* genes as well as untranslated regions (UTR). For *ITGA2B* we sequenced 416bp upstream of the promoter and for *ITGB3* 463bp upstream. High-resolution melting curve analysis (HRM) was performed as described [Fiore et al., 2011].

Nomenclature

Human Genome Variation Society (HGVS) nomenclature is used throughout for cDNA and protein numbering unless otherwise stated. For nucleotide numbering, the A nucleotide of the ATG start codon was designated +1 (cDNA *ITGA2B* and *ITGB3* GenBank accession numbers NM_000419.3 and NM_000212.2, respectively). For amino acid numbering +1 corresponds to the initiating Met with signal peptide included. However, as the numbering for the mature protein was used for the crystal structure of αIIbβ3 [see Xiao et al. 2004; Zhu et al. 2013], HGVS nomenclature is followed by mature protein numbering (in parentheses) in sections showing the influence of missense mutations on protein structure. This involves subtracting 31 amino acids from the HGVS numbering of αIIb and 26 amino acids for β3.

Minigene constructions and splicing analysis

Minigene constructs containing a genomic fragment spanning from the exon upstream to the exon downstream of the exon under study were synthesized by Epoch Life Science (Missouri, TX) and cloned into the Exontrap plasmid (MoBiTec GmbH, Goettingen, Germany). COS-7 cells were grown at $8x10^4$ cells/well in a 12-well plate with 1 ml of Dulbecco's modified Eagle's medium (Invitrogen, Carlsbad, CA, USA) supplemented with 10% fetal bovine serum, penicillin/streptomycin and 1M HEPES (Lonza, Verviers, Belgium) at 37°C in 5% CO_2. Wild-type and mutant minigene constructs were transiently transfected into cells 24 h later using the jetPRIME transfection reagent according to the manufacturer's instructions (Polyplus-transfection SAS, Strasbourg, France). Cells were then incubated for 48 h before isolation of total RNA using TRI Reagent (Molecular Research Center, Inc., Cincinnati, OH). cDNA was synthesized using 2 µg of RNA with the M-MLV reverse transcriptase kit (Promega corporation, WI, USA) and amplified with specific primers using different cycling programs (available on request). The amplified products were then resolved on 2% agarose gels and sequenced on a CEQ 8000 Genetic Analysis System using the CEQ DTCS Quick Start Kit (Beckman Coulter, Fullerton, CA, USA). Real-time PCR was carried out in a LightCycler 96 detection system (Roche Diagnostics, Mannheim, Germany) using intercalation of SYBR green as a fluorescence reporter.

Large gene deletions or duplications

To identify large homozygous or heterozygous deletions, or duplications, we used a relative quantitative real-time PCR assay. This approach was applied to 3 groups of patients: those for whom sequencing the *ITGA2B* or *ITGB3* genes revealed no genetic abnormality, a single heterozygous defect or a homozygous mutation but with no consanguinity described in the family. Exons of *ITGB3* and *ITGA2B* genes were amplified in a single amplicon (excepting for exon 1 of *ITGB3* which failed to amplify). Primers were designed using one-line primer-blast software (http://www.ncbi.nlm.nih.gov/tools/primer-blast/). PCR product sizes were about 200 bp. Melting curves were performed to verify the specificity of PCR products. Primer sequences and PCR protocols are available on request. Real time PCRs were performed on a Rotor-Gene 6000 cycler (Qiagen) in 20 µl volume, using QuantiTect® SYBR® Green PCR kit (Qiagen) with 5 ng of sample genomic DNA and 15 pmoles of each primer. First denaturation was performed at 95°C for 15 min, followed by 40 cycles (95°C for 15 sec, annealing temperature at 60°C for 15 sec, and 72°C for 20 sec). PCR reactions were terminated by a post-extension step of 90 sec at 72°C followed by a melting curve from 60 to 95°C (1 °C by step). Each patient was examined in triplicate in the same run. The relative amount of *ITGA2B* or *ITGB3* was established as a ratio of the reference gene, a 188 bp PCR product of *HMBS* (hydroxymethylbilane synthase, 11q23.3). We used a 2 Standard Curves method (Rotor-Gene Q series software 1.7.94: 2 Standard Curves Relative Quantification). The relative concentration is 1 when there is no rearrangement; 0.5 for a heterozygous deletion; 1.5 for a heterozygous duplication; and 2 for a homozygous duplication.

Site-directed mutagenesis and expression in heterologous cells

cDNAs of αIIb and β3 in pcDNA3 vectors were generously provided by Dr N. Rosenberg (Thrombosis and Hemostasis Institute, Sheba Medical Center, Israel). Mutations were introduced in full-length *ITGA2B* or *ITGB3* cDNA with the QuickChange II XL site-directed mutagenesis kit (Agilent Technologies, Santa Clara, CA) according to the manufacturer's instructions. COS-7 cells were cultured as described above. Cells were harvested 24 or 48 h after transfection and expression of cell surface αIIbβ3 assessed by flow cytometry with a Becton Dickinson (BD) Accuri™ C6 flow cytometer (BD Biosciences, Oxford, UK) using fluorescein isothiocyanate (FITC) conjugated anti-CD41/P2, anti-CD41/SZ22 (Beckman Coulter, Brea, CA), and anti-CD61 (Dako, Glostrup, Denmark) monoclonal antibodies (MoAbs) or as previously described by us [Milet-Marsal et al., 2002]. The activation state of recombinant αIIbβ3 was assessed by PAC-1 (BD Biosciences, Oxford, UK) binding after incubation of the cells with 1 mM $MnCl_2$. Transfected COS-7 cells were lysed in buffer containing sodium dodecyl sulfate (SDS) according to our standard procedures. SDS-polyacrylamide gel electrophoresis (SDS-PAGE) was performed using 10% gradient gels, in the presence or absence of 1mM dithiothreitol and proteins transferred to nitrocellulose. Bands corresponding to αIIb and β3 were located using the MoAbs SZ22 (αIIb, Beckman Coulter) and Y2/51 (β3, Dako, Glostrup, Denmark), with bound IgG assessed by chemiluminescence using peroxidase-linked anti-mouse IgG.

Protein Modeling

Models were constructed using the PyMol Molecular Graphics System, version 1.3, Schrödinger, LLC (www.pymol.org) and 3fcs or 2vdo pdb files for crystal structures of αIIbβ3 in the bent or extended conformations and 2knc pdb files for transmembrane and cytosolic domains as described in our previous publications [Nurden et al., 2011; 2013]. Amino acid changes are visualized in the rotamer form showing side change orientations incorporated from the Dunbrack Backbone library with the maximum probability.

Molecular dynamics simulations

These were performed as described by us [Laguerre et al., 2013]. Briefly, our procedure starts from the X-ray structure of αIIbβ3 with pdb code 3NIG (resolution 2.25 Å) using αIIbβ3 truncated at membrane proximal domains. Calculations were accomplished using GROMACS 4.5 and the GROMOS96 force field (G43a1) packages. Molecular dynamics runs were performed at constant temperature and pressure with a Berendsen coupling algorithm [Laguerre et al., 2013]. The αIIb mutant p.Gly44Val was created via the appropriate module in Discovery Studio version 3.1. In trajectory analyses root mean square deviations (RMSD) were calculated on Calpha positions.

Results

Patients' phenotype

The phenotypes of 83 GT patients grouped within 76 families are given in Supp. Table S1. The majority of families (58) have type I GT with <5% αIIbβ3 on their platelets. In agreement with the report of 64 cases by George et al. [1990], lesser but significant subpopulations of families have type II (9 families; 5 to 25% αIIbβ3) or potential variant forms with qualitative defects (8 families, 25% to 100% αIIbβ3). For one patient (GT76) αIIbβ3 was not assessed. Symptoms included epistaxis, easy bruising, hematomas, ecchymoses, petechiae, gingivorrhagia, post-invasive bleeding, heavy bleeding at menarche and/or menometrorrhagia; 23 patients (28%) had experienced GI bleeding (often a major problem in later life). Hemarthroses and intracranial bleeding were very rare. Details of treatment were unavailable for 6 patients while 8 patients had received no treatment or were restricted to anti-fibrinolytics or local measures. A large majority of patients for whom details were available had received one or more transfusions of platelet (74%) or RBC (70%) concentrates and/or rFVIIa (39%) in response to heavy bleeding or as a preventive measure prior to surgical trauma or childbirth. While most patients exhibited bleeding from early age, GT was occasionally diagnosed late in life with bleeding first occurring after trauma or, for women, at childbirth. Variability was seen even within the same family (see GT36a-c). Each patient was retrospectively assigned a bleeding score (1 to 4) according to WHO guidelines (see Section genotype/phenotype correlations).

Patients' genotype

Supp. Table S2 identifies sequencing variants absent from the NIH dbSNP database and considered candidates causal of GT by computer-based algorithms or following *in vitro* testing. A second sequencing and/or HRM analysis confirmed each variation after a new PCR amplification from DNA of the propositus and/or family members. The wide distribution of mutations across both genes is shown in Fig. 1 and their relative proportion by type in Supp. Fig. S1 (part A). Splice site, frameshift (and small deletions or duplications), missense and nonsense mutations were all common. Of the 78 different genetic variants, 55 were novel to this study; previously reported mutations are referenced in Supp. Table S3. When possible, segregation of mutations in affected families was confirmed by HRM analysis or direct sequencing; HRM is illustrated for the parents of GT41 in Supp. Fig. S2. Of the above mutations, eleven were repeated at least once among the 76 families included in our study (Fig. 1).

Homozygous mutations occurred in 27 of the 76 families (16 affecting *ITGA2B* and 11 *ITGB3*) for which a high proportion (63%) associated with consanguinity (not known for two families). Included are two siblings of a Moroccan family (GT43a and b) homozygous for c.614+1G>T splice and c.683G>A (p.Arg228His) variants of *ITGB3*. HRM analysis and sequencing confirmed that each parent carried the two mutations on a single allele. This family is from a remote region in Morocco and inbreeding over generations is highly probable. A total of 30 families showed compound heterozygosity (affecting *ITGA2B* for 20 patients and *ITGB3* for 10 patients). Two families (GT3 and GT35) had three potential damaging heterozygous mutations while GT35 had potentially damaging mutations in both genes. Sequencing identified only a single heterozygous mutation in 7 families (5 *ITGA2B* and 2 *ITGB3*). These included 4 patients with platelets expressing <5% αIIbβ3, one with type II GT and two patients with possible variant GT (GT4 and GT73). No mutations were located

for 12 patients including 7 whose platelets had <5% αIIbβ3 expression and 5 whose phenotype suggested variant GT (GT2, GT16, GT17, GT29 and GT46).

Two patients from Bordeaux, for whom PCR-SSCP screening had previously identified single heterozygous mutations: GT9: *ITGB3,* p.Leu222Pro (L196P in classic numbering for the mature protein) and GT10: *ITGA2B,* p.Arg1026Gln (R996Q) [Peyruchaud et al. 1998; Nurden et al. 2002]; were now shown as compound heterozygotes for mutations in *ITGB3* and *ITGA2B* respectively, thereby underlining the relative inefficiency of PCR-SSCP for mutation detection.

Missense mutations

Of the 22 missense mutations affecting *ITGA2B,* 13 concerned the αIIb N-terminal β-propeller encoded by exons 1 to 13, with 2 in the thigh domain, 6 in the membrane proximal calf-1 and calf-2 domains and 1 previously identified mutation in the cytoplasmic domain (Fig. 1; Supp. Fig S1). Of the 16 missense mutations affecting *ITGB3*, all were extracellular with 4 in the N-terminal PSI and hybrid domains, 7 in the βI domain and 4 in the EGF domains while 1 localized to the signal peptide.

(a) Mutations affecting the β-propeller region of αIIb. Our results confirm that missense mutations modifying the β-propeller of αIIb are a frequent cause of GT. Of the 13 that we located in this region, 8 were novel (Fig. 1, Supp. Table S2). Most affected were the highly conserved structures. Homozygous amino acid substitutions included p.Gly201Ser common to two families from Argentina (GT52, GT58) and p.Arg358His in a French patient (GT26) that re-appeared in heterozygous form in a German family (GT11). Heterozygous missense mutations in the β-propeller were associated with other missense mutations in the β-propeller, in the calf-2 domain, or with splice site mutations or frameshifts. Three families

with β-propeller mutations had type II GT with significant residual αIIbβ3 expression (GT11, GT18 and GT55) while the remainder had type I GT with <5% αIIbβ3.

Figure 2 highlights structural modifications induced by selected novel amino acid substitutions in β-propeller conserved motifs. It is noteworthy that p.Gly44Val (G13V), p.Gly201Ser (G170S), p.Ala216Val (A185V) and p.Gly321Trp (G290W) all affect FG-GAP motifs modifying β-propeller structure at the interface with β3. The p.Gly44Val change in blade 7 causes steric interference between the first two β-strands leading to their separation (shown at increased resolution in Supp. Fig. S3 parts A,B); the tight interaction between these two β-strands is important for the locking of the β-propeller structure. It may also disrupt Ca^{2+}-binding and potentially affect N-glycosylation at Asn46 (N15). Molecular dynamics simulations confirmed increased instability of the substituted αIIb β-propeller, with a dramatic Ca^{2+}-dependent increase of RMSD (Supp. Fig. S3 part C). The changes caused a block in αIIbβ3 biosynthesis; WB confirmed the absence of αIIb in platelets (Supp. Table S1). The p.Gly201Ser (G170S), p.Ala216Val (A185V) and p.Gly321Trp (G290W) substitutions influence H-bonding and blade structure. Hydrophobic amino acids are enriched in the blades, notably for the central antiparallel β-sheet. The exclusion of water molecules protects lateral H-bonds that bind and organize the four anti-parallel β-sheets. The p.Val286Asp (V255D) substitution introduces a polar structure in this hydrophobic environment, promoting destabilization by opening the angle between blades 3 and 4 (Fig. 2). Water molecules enter and competitively form H-bonds with oxygen atoms or NH_2-groups of constituent amino acids and disrupt structure. The p.Val420Ala (V389A) change promotes destabilization by pushing apart blades 6 and 7 (not illustrated). In contrast, p.Gly401Cys (G370C) alters local electrostatic potential and affects a Ca^{2+}-binding loop by disrupting a H-bond with a nearby Asp in a conserved motif that binds Ca^{2+}.

(b) Mutations affecting the αIIb thigh and calf domains. Eight missense mutations in our cohort affect these domains (Fig. 1), of these only p.Gln626His (Q595H), p.Cys705Arg (C674R), and p.Val934Phe (V903F) are known (Supp. Table S3). In our cohort, p.Val934Phe was heterozygous in a type II French patient (GT18) where it combines with p.Gly401Cys. It also occurs as the only affected allele in a second French patient with 10-20% residual αIIbβ3 (GT20) pointing to the presence of a second as yet undiscovered genetic defect. All other patients in this cohort had type I GT. The substitution p.Cys705Arg in a type II patient (GT49) was originally described in a Spanish type II GT patient where it disrupted an intramolecular Cys705-Cys718 disulfide blocking pro-αIIbβ3 maturation [Gonzalez-Manchon et al., 1999]. Molecular modeling is illustrated in Fig. 3 for the novel p.Gly823Glu (G792E), p.Leu955Gln (L924Q), and p.Thr984Lys (T953K) mutations located in GT27, GT21 and GT72 respectively. Gly823 (G792) is found between calf-1 and calf-2 in an unstructured connecting loop between two adjacent β sheets. The larger negatively charged Glu increases the angle between the two domains by pushing away the connecting ribbon between calf-1 and calf-2 with a straightening of the second distal part of the long arm of αIIb. In vitro mutagenesis confirmed a reduced surface expression with wild-type β3 in COS-7 cells and a high proportion of intracellular pro-αIIbβ3 in the cells (data not shown). The p.Leu955Gln (L924Q) and p. Thr984Lys (T953K) substitutions are adjacent to a conserved calf-2 sequence consisting of five polar amino acids orientated towards the inside of the β-barrel structure of calf-2 and held in place by H-bonds; they introduce steric encumbrance breaking H-bonds with loss of rigidity within the calf-2 structure.

(c) Mutations within exons of ITGA2B interfering with splicing. Included among the missense mutations are homozygous p.Gln626His (GT69) and heterozygous p.Phe191Val (GT57) substitutions; however, the causative nucleotide transitions within exons 18 and 4 respectively are predicted to interfere with splicing. The c.1876G>C (p.Gln626His) transition

was shown to result in skipping of exon 18 by Jallu et al. [2010] and was not studied further. The c.571T>G (p.Phe191Val) mutation is novel and NNSPLICE no longer identified the normal donor splice site of intron 4 in the mutant; all prediction tools found a new potential splice site 4 bp upstream of the natural donor splice site in intron 4 with elevated scores (SSF, 75.45; NNSPLICE, 0.75; HSF, 82.35). We confirmed this prediction by expressing a mutated minigene covering this region in COS-7 cells. While PCR amplification showed similar sized products for the wild type and mutated fragment (Fig. 4 panel A), sequencing revealed that the most common mutated transcript contained a four bp deletion (TTTA) that introduced a frameshift and a premature stop codon after 39 amino acids.

(d) Missense mutations affecting β3. A total of 15 missense mutations occurred in the extracellular domains of β3 while another (p.Trp11Arg) (found in GT62) affected the signal peptide (Fig. 1; Supp. Table S2). Six homozygous mutations all associated with type I GT while heterozygous mutations occurred in families with type I, type II or variant GT. The majority of the β3 missense mutations are novel: only p.Arg119Gln (R93Q), p.Leu222Pro (L196P), p.Cys601Arg (C575R) and p.Cys624Tyr (C598Y) have been previously reported. The physiologic importance of p.Arg119Gln (GT53) that also disrupts the HPA-1a epitope is controversial [Watkins et al., 2002; Peretz et al., 2006].

A novel heterozygous p.Arg63Cys (R37C) substitution in the PSI domain in a type II French patient (GT7) is of interest. This polar amino acid is adjacent to Cys39 (C13) in the PSI domain; Cys39 (C13) forms a long-range disulfide to Cys461 (C435) in the EGF-1 domain while the nearby Cys52 (C26) is linked to Cys75 (C49). The introduction of Cys63 introduces less steric encumbrance and possible disulfide exchange with nearby cysteines, most probably with Cys52 in view of its close proximity, a rearrangement that would destroy a loop essential for the hybrid domain structure (Fig. 5). To confirm the effect of p.Arg63Cys on the biogenesis of αIIbβ3, we transiently expressed mutant integrin in COS-7 cells. FACS

analysis showed 85% reduction of αIIbβ3Cys63 expression on transfected cells compared to wild type (Supp. Fig. S4). Immunoblotting of lysed cells showed a conspicuous presence of pro-αIIb and mature αIIb was reduced implying a slow or impaired αIIbβ3 complex maturation in this type II patient.

Two novel mutations affected the hybrid domain composed of β-sheets forming a β-barrel structure, the bulk of the hydrophobic amino acids orientating towards the interior (Fig. 5). Molecular modeling predicted that p.Leu118His (L92H) located in GT3 introduces instability not only through increased steric encumbrance but also by perturbing the hydrophobic environment. Arg131 (R105) (GT35a, b) is at the apex of a β-strand on the upper edge of the hybrid domain. The introduction of a Pro introduces a bend just before the segment that joins the βI domain. We detected 4 novel mutations in the βI domain (Fig. 5). The p.Pro189Ser (P163S) change, previously studied by us [Laguerre et al., 2013], influences Arg287 (Arg261), an amino acid of β3 that penetrates deep within the core of the αIIb β-propeller. Homozygous in a type I French patient (GT12), p.Pro189Ser is associated with a frameshift mutation in a second unrelated type I French patient (GT5). Homozygous p.Asp314Tyr in another type I patient (GT6) acts directly on the small β-helix 3-10 carrying Arg287. The p.Gly297Arg (G271R) substitution (GT73) introduces steric encumbrance at the interface between the αIIb and β3 headpieces. A homozygous p.Tyr344Ser (Y318S) mutation in GT23 with type I GT is localized near the β3 MIDAS site and adjacent to Asp277 (D251), Tyr344 forming a H-bond with an oxygen atom of the main chain of Asp277. Replacement of Tyr344 by the smaller Ser causes the loss of this H-bond rendering the segment containing the MIDAS and SyMBS sites less stable.

GT9 with type II GT and αIIbβ3 expression that almost borderlines with variant GT combines a previously reported heterozygous p.Leu222Pro (L196P) substitution with a second previously described activating β-propeller p.Cys624Tyr (C598Y) mutation that after transfection in CHO cells severely reduced but did not abrogate β3 expression [Chen et al., 2001; Nurden et al., 2002].

A heterozygous p.Asp578Asn mutation (GT3) caused by a nucleotide transition in exon 11 occurs after a two bp del in exon 5 of the same allele. Sequencing and HRM analyses for the patient's daughter confirmed their heterozygous presence on a single allele. As the latter is predicted to give a frameshift followed by a premature stop codon, the missense mutation may be an innocent bystander. The same remark applies to p.Arg228His in exon 5 that co-expressed with a c.614+1G>T transition affecting the splice site of exon 4 in the Moroccan family (GT43) with two linked homozygous mutations.

Splice site variations, frameshifts and stop codons

Stop codons leading to truncated subunits, often associated with nonsense-mediated decay were abundant (8 in *ITGA2B* and 2 *ITGB3*) but have been largely studied in GT [Peretz et al, 2006; Jallu et al. 2010] and were not explored further by us. A total of 15 different genetic variants affected intronic splice sites with 9 in *ITGA2B* (7 novel) and 7 in *ITGB3* (7 novel) (Supp. Table S2, Supp. Fig. S1). These included c.1544+1G->A at the splice donor site of intron 15 of *ITGA2B*, a mutation characteristic of the French Manouche gypsy tribe [Schlegel et al., 1995; Fiore et al., 2011]. This results in a premature stop codon leaving αIIb truncated before the transmembrane domain and type I GT. Two gypsy patients in our cohort (GT19, GT24) were homozygous for this mutation. A third (GT4) combined heterozygous expression with 50% platelet αIIbβ3 that proved nonfunctional due to a homozygous *FERMT3* (encoding kindlin-3) mutation [Robert et al., 2011]. Other mutation types in noncoding regions gave rise

to frameshifts (7 *ITGA2B*, 7 *ITGB3*) following small deletions or duplications and there was 1 UTR mutation. Splice site variations or insertion/deletion mutations mostly resulted in frameshifts and premature stop codons; exceptions are the in-frame variants seen for GT8 (presented below), GT15, GT38 and GT45, and two already known mutations found for GT50 and GT69. Exon skipping was predicted for the homozygous c.1879-2A>G (GT66, exon 19), c.2348+5G>C (GT8, exon 23) and the heterozygous c.574+1G>A (GT65, exon 4) variants of *ITGA2B;* and for the homozygous (c.614+1G>T (GT43, exon 4), c.777+1G>A (GT30, exon 5), c.613_614+2del (GT70, exon 4), and the heterozygous c.940-2A>G (GT38, exon 7) and c.2014+5G>A (GT54, exon 12) variants of *ITGB3* (Supp. Table S2). Two mutations were explored in more detail.

(i) A 13 bp del within intron 14 of ITGA2B. Intriguingly the most recurrent noncoding mutation is a heterozygous c.1440-13_c.1440-1del within intron 14 of *ITGA2B* in 7 families (Supp. Table S2). As these include patients from different countries with no obvious ancestral link, the most probable cause is a mutational hotspot although this is not readily apparent. To confirm activation of a cryptic splice site [Pillois et al., 2012], splicing patterns associated with this 13bp del were evaluated using the hybrid minigene transfection assay in COS-7 cells (Fig. 4). Results confirmed a new cryptic 5' splicing site and a 2-bp deletion within the mRNA. This induced a reading-frame shift and a premature stop codon after 105 aberrant amino acids. The abnormal mRNA produced is predicted to be a target for nonsense-mediated decay.

(ii) In vitro analysis of the c.2348+5G>C transversion in ITGA2B. Splicing tools predicted this variation in intron 23 of a type II patient (GT8) to result in the loss of a native splice site and skipping of exon 23, while maintaining the open reading frame. In all cases there was a loss or significant reduction of the splicing score of the natural splice donor site of exon 23 (SSF, 81 to 0; NNSPLICE, 0.63 to 0; Genesplicer 6.91 to 3.53 and HSF, 90.69 to

78.53). Skipping of exon 23 was confirmed experimentally using the hybrid minigene transfection assay (Fig. 4). Furthermore, using real-time PCR and primers specific for exons 22 and 23 or exon 22 to 24, we showed major quantitative changes in the expression of the spliced mRNAs (Supp. Fig. S5). A small residual expression of the normal transcript using primers for exon 22-23 may explain the residual αIIbβ3 on the platelet surface. Exon 23 codes for residues 756–783 of the αIIb subunit. To confirm the effect of this deletion on αIIbβ3 synthesis, we co-transfected an αIIb-ΔE23 cDNA construct into COS-7 cells with normal β3 cDNA. WB showed that cells transfected with normal αIIb displayed both pro-αIIb and mature αIIb, those transfected with αIIb-ΔE23 only expressed the mutated immature protein and there was no surface expression of mutated αIIbβ3 (Supp. Fig. S4).

A homozygous mutation (c.165T->C) mutation affecting the 3'-UTR of *ITGA2B* in a French patient of African origin with type I GT was not studied further as the patient (GT75) was no longer available.

Large gene deletions or rearrangements

A feature of our study was the search for large gene deletions or rearrangements in patients for whom single heterozygous or no gene mutations were detected by Sanger sequencing. The results are given in Supp. Table S2. Single allele deletions of exons 5 and 6 (GT45) and of exons 23 to 29 (GT68) were detected in *ITGA2B* while a deletion of exons 14 and 15 (GT54) was found in *ITGB3*. A homozygous duplication of exons 3-12 was also detected in *ITGA2B* of a Syrian patient (GT28). We also examined patients for whom homozygous mutations were found in the absence of reported consanguinity but no large gene deletions or rearrangements were found in this group.

Genotype/phenotype correlations

A preliminary examination of a breakdown of WHO bleeding score with respect to GT type showed a greater tendency for type I patients to have a higher bleeding score with respect to type II and the predicted variants who as groups tended to have a milder bleeding syndrome (Table 1). Notwithstanding, the number of type II patients remained small while the majority of patients predicted to have variant GT failed to genotype for *ITGA2B* or *ITGB3* defects in our study. Interestingly, for fully genotyped patients in the type I subgroup, bleeding severity was independent of the nature of the affected gene or of the type of mutation.

Discussion

Adapting the nomenclature of George et al. [1990], we classified patients into type I (<5% αIIbβ3), type II (5-25% αIIbβ3) or variants (>25% αIIbβ3). Only one patient (GT76) was included on the basis of a total absence of platelet aggregation alone. Sanger sequencing of *ITGA2B* or *ITGB3* provided an explanation for the GT phenotype in 57 families; 7 families (4 type I, 1 type II and 2 potential variants) had a single heterozygous mutation in *ITGA2B* or *ITGB3* and 12 families no mutations (7 type I and 5 potential variants). Of the 78 causative genetic variants, 55 were novel, confirming how outside ethnic groups most families possess their own private mutation. Novel heterozygous large deletions concerning two or more exons were subsequently detected by quantitative real-time PCR in 3 patients for whom a single heterozygous mutation had been revealed by Sanger sequencing; while a large homozygous duplication was located for GT28, a Syrian man with type I GT thus raising to 61 the families (80% of the total) for whom genotyping was successful. Previously, an inversion-deletion detected by Southern blot in a Mexican family with type I GT was linked to homologous recombination of intragene Alu sequences in *ITGB3* [Li and Bray, 1993].

Otherwise, reports of large deletions in *ITGA2B* or *ITGB3* are rare [Burk et al., 1991; Djaffar et al., 1993; Rosenberg et al., 1997]. Explanations for unsuccessful genotyping include defects (a) in non-sequenced intronic and upstream promoter regions, (b) of miRNA regulating αIIbβ3 synthesis and (c) in other genes that code for proteins necessary for αIIbβ3 synthesis or function.

Two patients with variant forms but with single or no mutations in *ITGA2B* or *ITGB3* were investigated further [Robert et al., 2011; Canault et al., 2014]. GT4 had heterozygous expression of the c.1544+1G>A French gypsy splice mutation but no platelet aggregation, results that contrast with obligate heterozygotes in GT where 50% αIIbβ3 expression allows normal platelet function [George et al., 1990]. As a moderate immune deficiency was associated with the severe bleeding phenotype, *FERMT3* responsible for leukocyte adhesion deficiency type III (LAD-III) was sequenced [Robert et al., 2011]. A novel homozygous A>C transversion in the exon 3 acceptor splice site of *FERMT3* led to a frameshift and a stop codon; a confirmed absence of kindlin-3 in platelets rendered the residual αIIbβ3 nonfunctional. For GT2, exome sequencing revealed a nonsynonymous c.G742T transversion in *RASGRP2* giving a p.Gly248Trp substitution in the CALDAG-GEFI signaling protein. In vitro expression showed a nonfunctional protein and a block in the Rap1-dependent activation pathway of αIIbβ3 but normal leukocyte function [Canault et al., 2014]. Genes involved in integrin-related signaling pathways clearly represent a previously unrecognized cause of variant GT and must be taken into account when considering phenotype.

Homozygous or compound heterozygous nonsense mutations all gave type I GT, findings compatible with a block in αIIbβ3 biogenesis and a high probability of nonsense-mediated mRNA decay [Vinciguerra et al., 1996; Arias-Salgado et al., 2002; Peretz et al., 2006; Jallu et al., 2010]. A specific example is the homozygous *ITGA2B* exon 19 c.1882C>T transition common to two Swiss siblings (GT39a/b) with type I GT. The result is a stop at

Arg628* (R597*), a mutation previously proven in a Spanish patient to prevent αIIbβ3 complex expression [Arias-Salgado et al., 2002]. The differing bleeding scores for the Swiss siblings emphasize how factors other than αIIbβ3 deficiency influence bleeding severity. Mutations affecting splice sites were abundant, concerned both genes and gave type I or type II GT. The c.1440-13_c.1440-1del in intron 14 of *ITGA2B* was enigmatic. Detected in 7 families spanning 3 European countries, the affected patients included all 3 siblings of a Catalan family (GT36) thus proving its inheritance. We confirmed experimentally that the use of a cryptic splicing site led to a 2-bp deletion within mRNA, a reading-frame shift and a premature stop codon after 105 aberrant amino acids. The abnormal mRNA is also predicted to be a target for nonsense-mediated decay. In all of our cases its presence segregates with a non-expressed allele. This 13-bp deletion is certainly that reported in patients from northwest France by Jallu et al. [2010] but who assigned it a slightly different nomenclature. The reasons for its repeated appearance in non-related European families or its restriction to a heterozygous state are unknown. It contrasts with a founder 13-bp in-frame deletion that is common in Palestinian–Arab patients and which leads to a deletion of 6 amino acids (Ala106-Gln111) within blade 2 of the αIIb propeller and a block in αIIbβ3 biogenesis [Rosenberg et al., 2005]. An interesting splice site mutation was the novel homozygous c.2348+5G>C transversion in *ITGA2B* in an elderly male type II patient (GT8) with severe bleeding in his youth and repeated GI bleeding in later life. In vivo experimentation allowed us to show that this mutation resulted in the skipping of exon 23 but that a small residual splicing of normal αIIb accounted for the residual αIIbβ3 in his platelets; significantly the presence of small amounts of αIIbβ3 did not protect against bleeding in his case.

We have highlighted 22 predicted damaging amino acid substitutions within αIIb and 16 in β3. A high proportion (13 with 9 novel) affect the αIIb β-propeller confirming earlier reports that many genetic variants causing GT disrupt this region [reviewed by Nelson et al., 2005; Mansour et al., 2011]. The β-propeller has 7 highly conserved blades each composed of 4 anti-parallel β-strands connected by loops; side domains associate with the βI domain of β3 while amino acid clusters on its upper surface contribute to ligand binding [Kamata et al., 2001; Podolnikova et al., 2014]. A key structural role is played by conserved FG-GAP repeats in each blade. Four Ca^{2+}-binding domains are present as part of β-hairpin loops extending from blades 4-7. Disease-causing β-propeller domain mutations either prevent pro-αIIbβ3 formation or, for the majority, interfere with trafficking of pro-αIIbβ3 from the ER to the Golgi. As shown by our study, amino acid substitutions in the β-propeller domain give primarily type I with also, on occasion, type II GT.

Our approach to β-propeller mutations was to look at the structural implications of novel amino acid substitutions highlighting those in conserved FG-GAP motifs. Molecular modeling showed how subtle changes and repositioning of side chains modified blade structure and H-bonding, particularly in domains affecting the interface with β3. Thus, the p.Gly44Val (GT39a-c) substitution in blade 7 disrupts β-sheet assembly, an instability that we confirmed experimentally by molecular dynamics simulations. The p.Gly44Val change may also interfere with N-glycosylation at Asn46, a key element in the binding of calnexin a chaperone, necessary for the transport of pro-αIIbβ3 to the Golgi apparatus [Mitchell et al., 2006]. The p.Gly201Ser change (GT52) disrupts H-bonding and is adjacent to a previously reported p.Phe202Cys substitution that causes loss of contact with β3Arg287 and prevents pro-αIIbβ3 formation [Rosenberg et al., 2004]. In contrast, p.Val286Asp (GT40) gives a more polar structure to the hydrophobic environment deep in the β-propeller allowing entry of water molecules that form disruptive H-bonds. A p.Ile405Thr mutation (GT74) in the αIIb

Ca^{2+}-binding domain, first characterized by Mitchell et al. [2003], creates increased electrostatic potential non-conductive for Ca^{2+} binding. A Ca^{2+}-binding loop is also the site of a novel p.Gly401Cys substitution (GT18) with disruption of a H-bond between Gly401 and a conserved Asp residue involved in metal ion binding. It is clear from the above and other reported mutations that the β-propeller is highly sensitive to the quality control exercised in the ER where mutated pro-αIIb or pro-αIIbβ3 are degraded by the proteasome.

We identified 8 missense mutations in the αIIb calf and thigh domains where less is known about αIIb structure. Previous studies have shown how a small deletion-insertion in calf-2 and an in-frame skipping of exon 20 affecting calf-1 failed to prevent pro-αIIbβ3 formation but interfered with maturation [Rosenberg et al., 2003]. Similar findings have been reported for a 21-amino acid deletion (Leu817-Gln837) in calf-2 and for p.Val982Met and p.His813Asn substitutions [Fujimoto et al., 2004; Nurden et al., 2004; Losonczy et al., 2007]. We focused on novel p.Gly823Glu, p.Leu955Phe and p.Thr984Lys mutations in calf-2. All were heterozygous in association with an identified and proven null mutation. Two gave type I GT (<5% αIIbβ3) (GT21, GT72), while p.Gly823Glu occurred in a French patient (GT27) with type II GT and 10% residual αIIbβ3 and where expression studies confirmed an altered maturation of pro-αIIbβ3. In fact, the larger negatively charged Glu823 results in the straightening of the second distal part of the long arm of αIIb. The p.Leu955Phe and p.Thr984Lys substitutions in calf-2 occur at or adjacent to a conserved motif of five polar amino acids central to the β-barrel protected from water molecules and involved in H-bond interactions. Both mutations induce flexibility. Finally, just how αIIb is under tight quality control is nicely shown for p.Cys705Arg (C674R in the mature protein) (GT49) where previous studies have shown that the mutated αIIb is retained by the BiP chaperone in the ER [Arias-Salgado et al., 2001].

Previously characterized missense mutations affecting β3 include variant GT with normally or partially expressed αIIbβ3 that fails to bind ligands when activated [Loftus et al., 1990; Bajt et al., 1992; Lanza et al., 1992]. In our study, missense mutations in β3 primarily interfered with αIIbβ3 biogenesis. A novel heterozygous p.Arg63Cys substitution in the N-terminal PSI domain of a type II French patient (GT7) is adjacent to Cys39 that forms a long-range disulfide with Cys461 in EGF-1 while nearby Cys52 joins with Cys75. Introduction of Cys at position 63 leads to possible disulfide exchange while in vitro expression studies showed altered pro-αIIbβ3 maturation. Interestingly, p.Cys39Gly and disruption of its long-range disulfide also gives GT [Peretz et al., 2006]. Clustered hybrid domain substitutions, p.Leu118His (GT3) and p.Arg119Gln (GT53), as well as p.Arg131Pro (GT35) all caused loss of αIIbβ3 expression with molecular modeling predicting changes in H-bonding. Specifically, the novel p.Arg131Pro on the upper edge of the hybrid domain introduces a bend just before the segment that joins the βI domain of β3.

Mutations in βI were associated in their majority with type I or type II GT and one potential variant form. Of these, molecular modeling shows that a homozygous p.Tyr344Ser mutation in GT23 leads to loss of a H-bond with Asp277 that potentially affects the MIDAS and SyMBS sites although the result is a loss of αIIbβ3 expression and type I GT. Both p.Pro189Ser and p.Asp314Tyr giving type I GT destabilize β3Arg287 an amino acid that penetrates deep within the core of the αIIb β-propeller, a finding previously shown by us for p.Pro189Ser by molecular dynamics simulation [Laguerre et al., 2013]. The p.Leu222Pro substitution differed in that it was associated with type II GT (GT9), a patient whose platelets fail to bind Fg (or PAC-1) on activation or to support clot retraction [Nurden et al., 2002]. Other βI domain mutations in the literature giving type II GT can lead to residual αIIbβ3 with conserved function [Ambo et al., 1998; Jackson et al., 1998; Ward et al., 2000]. Quite clearly,

βI-domain mutations can have widely diverging quantitative and qualitative effects on αIIbβ3 expression.

Four missense mutations localized to the disulfide-rich β3 EGF-3 and EGF-4 domains. Of these, p.Cys601Arg (GT60) disrupts a disulfide with Cys612; a mutation that was first characterized in type I GT in Italy [D'Andrea et al., 2002]. Disruption of EGF-domain disulfides leads to abrogated expression or to reduced activated forms [Mor-Cohen et al., 2012]. First located in type II GT [Chen et al., 2001], the activating p.Cys624Tyr substitution re-occurred in type II GT9 in combination with the loss of function p.Leu222Pro and in this situation spontaneous Fg- or PAC-1 binding to platelets was not seen (Supp. Table S1). β3 missense mutations can abrogate expression of both αIIbβ3 and αvβ3 receptors or have differential effects [Tadokoro et al., 2002; Mor-Cohen et al., 2012]. Indeed, β3 p.Pro189Ser common to GT5 and GT12 actually reinforces the interaction between αv and β3 while giving type I GT [Laguerre et al., 2013]. Heterozygous β3 p.Gly297Arg was the only mutation detected in GT73, a French woman with a severe bleeding syndrome and an absence of platelet aggregation but qualitatively abnormal αIIbβ3 (Supp. Table S1). This patient has a supposed second mutation that remains elusive and whose identification will be necessary to fully understand her phenotype.

The highly polymorphic nature of *ITGB3* and to a lesser extent *ITGA2B* is shown by the 33 human platelet alloantigen (HPA) systems spread across their extracellular domains [Curtis & McFarland, 2013]. In addition to homozygous disease-causing mutations, two unrelated French families (GT44, GT50) showed heterozygous expression of *ITGA2B* p.Val868Met (V837M in the mature protein) (data not shown). In fact, p.Val868Met is a low-frequency HPA that segregates with the HPA-3b allele [Peterson et al., 2014]. Low-frequency HPAs must be excluded when genotyping GT patients. Isoantibody formation following blood transfusion or during pregnancy is a major risk in GT [George et al., 1990;

Gruel et al., 1994]. In the current study, antibodies to αIIbβ3 have been detected in 20 patients (14 female, 6 male; Supp. Table S1). Of these, only one, a woman without children belonging to the French Manouche gypsy tribe (GT19) had not received platelet or RBC transfusions and the cause of her immunization remains unknown (Supp. Table S1). Eighteen of the immunized patients were type I GT reinforcing our recent conclusion from a smaller study that the risk of isoantibody formation is largely restricted to patients whose platelets lack αIIbβ3 on their surface [Fiore et al., 2012].

Striking from our study is the conclusion that the bleeding severity for the fully genotyped type I patients is independent of the affected gene (Table 1). While the chances of a severe bleeding phenotype are greater for a type I patient, there were exceptions with both type II patients (e.g. GT8) and variants (e.g. GT4) with a lifelong disorder severely impairing quality of life. In this initial analysis of our data we used a simple WHO bleeding score questionnaire. We now plan to perform a more intense analysis of the clinical data taking more precisely into account such variables as the number of bleeding episodes and the age of the patient, the number of transfusions, the number of RBC concentrates and also the country of origin. We will also be able to include other type II patients and variants from outside our cohort to make for a more powerful statistical analysis of their phenotype severity. But it is already quite clear that GT contrasts, for example, with MYH9-related disease (MYH9-RD) where the *MYH9* genotype is a major determinant of the clinical manifestations allowing a hierarchical prognostic model [Saposnik et al., 2014]. In MYH9-RD, mutations and deficiency or nonfunctioning of nonmuscle myosin IIA are variably associated with kidney disease, deafness and cataracts and their appearance and severity can vary with the location and nature of the causative mutation. In contrast, in GT despite the expression of β3 in many lineages, the primary phenotype remains mucocutaneous bleeding due to a loss of platelet function. Significantly, although GI bleeding is a major problem especially in later life, 10

affected patients had *ITGA2B* compared to 8 with *ITGB3* defects suggesting that αvβ3 is not involved. Although residual integrin in type II GT may be protective, for some patients the αIIbβ3 may have retained only partial or no functional capacity. While in variant GT-like syndromes genes involved in regulating αIIbβ3 function may give specific phenotypes; the phenotypic variability in classic GT appears likely to depend on epidemiological and other genetic factors affecting coagulation or vascular pathways of hemostasis. Large studies such as ours will allow follow-up studies to identify these factors in genotyped families.

Acknowledgments

We especially thank Dr. Michel Laguerre for the molecular dynamics simulations and acknowledge the role played by Dr. Marta Pico in patient recruitment from Spain. Dr. Pico died in the summer of 2011 after a long illness and ATN dedicates this work to her.

Conflict of Interest. All authors state that they have no conflicts of interest concerning the contents of this manuscript.

References

Ambo H, Kamata T, Handa M, Taki M, Kuwajima M, Kawai Y, Oda A, Murata M, Takada Y, Watanabe K, Ikeda Y. 1998. Three novel integrin β3 subunit missense mutations (H280P, C560F, and G579S) in thrombasthenia. Including one (H280P) prevalent in Japanese patients. Biochem Biophys Res Commun 251:763-768.

Arias-Salgado EG, Butta N, Gonzalez-Manchon C, Ayuso MS, Parrilla R. 2001. Competition between normal (674C) and mutant (674R)GPIIb subunits: role of the molecular chaperone BiP in the processing of GPIIb-IIIa complexes. Blood 97:2640-2647.

Arias-Salgado EG, Tao J, Gonzalez-Manchon C, Butta N, Vivente V, Avuso MS, Parilla R. 2002. Nonsense mutation in exon-19 of GPIIb associated with thrombasthenic phenotype. Failure of GPIIb(delta597-1008) to form stable complexes with GPIIIa. Thromb Haemost 87:684-691.

Bajt ML, Ginsberg MH, Frelinger AL 3rd, Berndt MC, Loftus JC. 1992. A spontaneous mutation of integrin alphaIIbbeta3 (platelet GPIIb-IIIa) helps define a ligand-binding site. J Biol Chem 267:3789-3794.

Bercovitz RS, O'Brien SH. 2012. Measuring bleeding as an outcome in clinical trials of prophylactic platelet transfusions. Hematology Am Soc Hematol Educ Program 2012:157-60. Doi: 10.1182/asheducation-2012.1.157.

Burk CD, Newman PJ, Lyman S, Gill J, Coller BS, Poncz M. 1991. A deletion in the gene for glycoprotein IIb associated with Glanzmann's thrombasthenia. J Clin Invest 87:270-276.

Canault M, Ghalloussi D, Grosdidier C, Guinier M, Perret C, Chelgoum N, Germain M, Raslova H, Peiretti F, Morange PE, Saut M, Pilloix X, et al. 2014. A CALDAG-GEFI gene (RASGRP2) mutation affects platelet function and causes severe bleeding in man. J Exp Med 211:29621-29632.

Chen YP, Djaffar I, Pidard D, Steiner B, Cieutat AM, Caen JP, Rosa JP. 1992. Ser752->Pro mutation in the cytoplasmic domain of integrin beta3 subunit and defective activation of platelet integrin alphaIIbbeta3 (glycoprotein IIb-IIIa) in a variant of Glanzmann thrombasthenia. Proc Natl Acad Sci USA 89:10169-10173.

Chen P, Melchior C, Brons NH, Schlegel N, Caen J, Kieffer N. 2001. Probing conformational changes in the I-like domain and the cysteine-rich repeat of human beta3 integrins following disulfide bond disruption by cysteine mutations: identification of cysteine 598 involved in alphaIIbbeta3 activation. J Biol Chem 276:38268-38635.

Choi WS, Rice WJ, Stokes DL, Coller BS. 2013. Three-dimensional reconstruction of intact human integrin αIIbβ3: new implications for activation-dependent ligand binding. Blood 122:4165-4171.

Coller BS, Shattil SA. 2008. The GPIIb/IIIa (integrin αIIbβ3) odyssey: a technology-driven saga of a receptor with twists, turns, and even a bend. Blood 112:3011-3025.

Curtis BR, McFarland JG. 2013. Human platelet antigens – 2013. Vox Sang 106:93-102.

D'Andrea G, Colaizzo D, Vecchione G, Grandone E, Di Minno G, Maraglione M; Glanzmann's Thrombasthenia Italian Team (GLATIT). 2002. Glanzmanns thrombasthenia: identification of 19 new mutations in 30 patients. Thromb Haemost 87:1034-1042.

Djaffar I, Caen JP, Rosa JP. 1993. A large deletion in the human platelet glycoprotein IIIa (integrin beta 3) gene associated with Glanzmann's thrombasthenia. Hum Mol Genet 2:2183-2185.

Eng ET, Smagghe BJ, Walz T, Springer TA. 2011. Intact αIIbβ3 integrin is extended after activation as measured by solution x-ray scattering and electron microscopy. J Biol Chem 286:35218-35226.

Fiore M, Pillois X, Nurden P, Nurden AT, Austerlitz, F. 2011. Founder effect and estimation of the age of the French gypsy mutation associated with thrombasthenia in Manouche families. Eur J Hum Genet 19:981-987.

Fiore M. Firah N, Pillois X, Nurden P, Heilig R, Nurden AT. 2012. Natural history of platelet antibody formation against αIIbβ3 in a French cohort of Glanzmann thrombasthenia patients. Haemophilia 18:e201-209.

Fujimoto T-T, Sora M, Ide K, Mizushima M, Mita M, Nishimura S, Ueda K, Fujimura K. 2004. Glanzmann thrombasthenia associated with a 21-amino acid deletion (Leu817-Gln837) in glycoprotein IIb due to abnormal splicing in exon 25. Int J Haematol 80:83-90.

George JN, Caen JP, Nurden AT. 1990. Glanzmann's thrombasthenia: The spectrum of clinical disease. Blood 75:1383-1395.

Gonzalez-Manchon C, Fernandez-Pinal M, Arias-Salgado EG, Ferrer M, Alvarez M-V, Garcia-Munoz S, Ayuso MS, Parilla R. 1999. Molecular genetic analysis of a compound heterozygote for the glycoprotein (GP) IIb gene associated with Glanzmann's thrombasthenia: disruption of the 674-687 disulfide bridge in GPIIb prevents surface exposure of GPIIb-IIIa complexes. Blood 93:866-875.

Gruel Y, Brojer E, Nugent DJ, Kunicki TJ. 1994. Further characterization of the thrombasthenia-related idiotype OG. Antiidiotype defines a novel epitope(s) shared by fibrinogen B beta chain, vitronectin and von willebrand factor and requied for binding to beta 3. J Exp Med 180:2259-2267.

Jackson DE, White MM, Jennings LK, Newman PJ. 1998. A Ser162->Leu mutation within glycoprotein (GP) IIIa (integrin β3) results in an unstable αIIbβ3 complex that retains partial function in a novel form of type II Glanzmann thrombasthenia. Thromb Haemost 80:42-48.

Jallu V, Dusseaux M, Panzer S, Torchet MF, Goudemand J, de Brevern AG, Kaplan C. 2010. AlphaIIbbeta3 integrin: new allelic variants in Glanzmann thrombasthenia, effects on ITGA2B and ITGB3 mRNA splicing, expression, and structure-function. Hum Mutat 31:237-246.

Kamata T, Tieu KK, Irie A, Springer TA, Takada Y. 2001. Amino acid residues in the αIIb subunit that are critical for ligand binding to integrin αIIbβ3 are clustered in the β-propeller. J Biol Chem 276: 44275-44283.

Kannan M, Ahmad F, Yadav BK, Kumar R, Choudhry VP, Saxena R. 2009. Molecular defects in ITGA2B and ITGB3 genes in patients with Glanzmann thrombasthenia. J Thromb Haemost 7:1878-1885.

Laguerre M, Sabi E, Daly M, Stockley J, Nurden P, Pillois X, Nurden AT. 2013. Molecular dynamics analysis of a novel β3 Pro189Ser mutation in a patient with Glanzmann thrombasthenia differentially affecting αIIbβ3 and αvβ3 expression. PLoS One 8(11):e78683.doi: 10.1371.

Lanza F, Stierlé A, Fournier D, Morales M, André G, Nurden AT, Cazeenave J-P. 1992. A new variant of Glanzmann's thrombasthenia (Strasbourg I). Platelets with functionally defective glycoprotein IIb-IIIa complexes and a glycoprotein Arg214->Trp mutation. J Clin Invest 89:1995-2004.

Li L, Bray PF. 1993. Homologous recombination among three intragene Alu sequences causes an inversion-deletion resulting in the hereditary bleeding disorder Glanzmann thrombasthenia. Am J Hum Genet 53:140-149.

Loftus JC, O'Toole TE, Plow EF, Glass A, Frelinger II, AL, Ginsberg MH. 1990. A β3 integrin mutation abolishes ligand binding and alters divalent cation-dependent conformation. Science 249:915-918.

Losonczy G, Rosenberg N, Boda Z, Vereb G, Kappelmayer J, Hauschner H, Bereczky Z, Muszbek L. 2007. Three novel mutations in the glycoprotein IIb gene in a patient with type II Glanzmann thrombasthenia. Haematologica 92:698-701.

Mansour W, Einav Y, Hauschner H, Koren A, Seligsohn U, Rosenberg N. 2011. An αIIb mutation in patients with Glanzmann thrombasthenia located in the N-terminus of blade 1 of the β-propeller (Asn2Asp) disrupts a calcium binding site in blade 6. J Thromb Haemost 9:192-200.

Milet-Marsal S, Breillat C, Peyruchaud O, Nurden P, Combrié R, Nurden A, Bourre F. 2002. Two different beta3 cysteine substitutions alter alphaIIbbeta3 maturation and result in Glanzmann thrombasthenia. Thromb Haemost 88:104-110.

Mitchell WB, Li JH, Singh F, Michelson AD, Bussel J, Coller BS, French DL. 2003. Two novel mutations in the alphaIIb-calcium-binding domains identify hydrophobic regions essential for alphaIIbbeta3 biogenesis. Blood 101:2268-2276.

Mitchell WB, Li J, French DL, Coller BS. 2006. AlphaIIbbeta3 biogenesis is controlled by engagement of alphaIIb in the calnexin cycle via the N15-linked glycan. Blood 107:2713-2719.

Mor-Cohen R, Rosenberg N, Einav Y, Zelzion E, Landau M, Mansour W, Averbukh Y, Seligsohn U. 2012 Unique disulfide bonds in epidermal growth factor (EGF) domains of β3 affect structure and function of αIIbβ3 and αvβ3 integrins in different manner. J Biol Chem 287:8878-8891.

Nelson EJ, Li J, Mitchell WB, Chandy M, Srivastava A, Coller BS. 2005. Three novel beta-propeller mutations causing Glanzmann thrombasthenia result in production of normally stable pro-αIIb, but variable impaired progression of pro-αIIbβ3 from endoplasmic reticulum to Golgi. J Thromb Haemost 3:2773-2783.

Nurden AT, Ruan J, Pasquet JM, Gauthier B, Combrié R, Kunicki T, Nurden P. 2002. A novel 196Leu to Pro substitution in the beta3 subunit of the alphaIIbbeta3 integrin in a patient with a variant form of Glanzmann thrombasthenia. Platelets 13:101-111.

Nurden AT, Breillat C, Jacquelin B, Combrié R, Freedman J, Blanchette VS, Schmugge M, Rand ML. 2004. Triple heterozygosity in the integrin αIIb subunit in a patient with Glanzmann's thrombasthenia. J Thromb Haemost 2:813-819.

Nurden AT, Fiore M, Nurden P, Pillois X. 2011. Glanzmann thrombasthenia: a review of ITGA2B and ITGB3 defects with emphasis on variants, phenotypic variability, and mouse models. Blood 118:5996-6005.

Nurden AT, Pillois X, Wilcox DA. 2013. Glanzmann thrombasthenia: State of the art and future directions. Semin Thromb Hemost 39:642-655.

Peretz H, Rosenberg N, Landau M, Usher S, Nelson EJ, Mor-Cohen R, French DL, Mitchell BW, Nair SC, Chandy M, Coller BS, Srivastava A et al. 2006. Molecular diversity of Glanzmann thrombasthenia in southern India: new insights into mRNA splicing and structure-function correlations of alphaIIbbeta3 integrin (ITGA2B, ITGB3). Hum Mutat 27:359-369.

Peterson JA, Gitter M, Bougie DW, Pechauer S, Hopp KA, Pietz B, Szabo A, Curtis BR, McFarland J, Aster RH. 2014. Low-frequency human platelet antigens as triggers for neonatal alloimmune thrombocytopenia. Transfusion 54:1286-1293.

Peyruchaud O, Nurden AT, Milet S, Macchi L, Pannochia A, Bray PF, Kieffer N, Bourre F. 1998. R to Q amino acid substitution in the GFFKR sequence of the cytoplasmic domain of the integrin αIIb subunit in a patient with a Glanzman's thrombasthenia-like syndrome. Blood 92:4178-4187.

Pillois X, Fiore M, Heilig R, Pico M, Nurden AT. 2012. A novel amino acid substitution of integrin αIIb in Glanzmann thrombasthenia confirms that the N-terminal region of the receptor plays a role in maintaining β-propeller structure. Platelets 24:77-80.

Podolnikova NP, Yakovlev S, Yakubenko VP, Wang X, Gorkun OV, Ugarova TP. 2014. The interaction of integrin αIIbβ3 with fibrin occurs through multiple binding sites in the αIIb β-propeller domain. J Biol Chem 289:2371-2383.

Robert P, Canault M, Farnarier C, Nurden A, Grosdidier C, Barlogis V, Bongrand P, Pierres A, Chambost P, Alessi MC. 2011. A novel Leukocyte Adhesion Deficiency III variant: kindlin-3 deficiency results in integrin and non-integrin-related defects in late steps of leukocyte adhesion. J Immunol 186:5273-5283.

Rosenberg N, Yatuv R, Zivelin A, Dardik R, Peretz H, Seligsohn U. 1997. Glanzmann thrombasthenia caused by an 11.2-kb deletion in the glycoprotein IIIa (beta3) is a second mutation in Iraqi Jews that stemmed from a distinct founder. Blood 89:3654-3662.

Rosenberg N, Yatuv R, Sobolev V, Peretz H, Zivelin A, Seligsohn U. 2003. Major mutations in calf-1 and calf-2 domains of glycoprotein IIb in patients with Glanzmann thrombasthenia enable GPIIb/IIIa complex formation but impair its transport from the endoplasmic reticulum to the Golgi apparatus. Blood 101:4808-4815.

Rosenberg N, Landau M, Luboshitz J, Rechavi G, Seligsohn U. 2004. A novel Phe171Cys mutation in integrin αIIb causes Glanzmann thrombasthenia by abrogating αIIbβ3 complex formation. J Thromb Haemost 2:1167-1175.

Rosenberg N, Hauschner H, Peretz H, Mor-Cohen R, Lansau M, Shenkman B, Kenet G, Coller BS, Awidi AA, Seligsohn U. 2005. A 13-bp deletion in αIIb is a founder mutation that predominates in Palestinian-Arab patients with Glanzmann thrombasthenia. J Thromb Haemost 3:2764-2772.

Saposnik B, Binard S, Fenneteau O, Nurden A, Nurden P, Hurtaud-Roux M-F, Schlegel N; French MYH9 network. 2014. Mutation spectrum and genotype-phenotype correlations in a large cohort of MYH9-related disorders. Mol Genet Genomic Med 2:297-312.

Schlegel N, Gayet O, Morel-Kopp MC, Wyler B, Hurtaud-Roux MF, Kaplan C, McGregor J. 1995. The molecular genetic basis of Glanzmann's thrombasthenia in a gypsy population in France: identification of a new mutation on the alphaIIb gene. Blood 86:977-982.

Seligsohn U. Treatment of inherited bleeding disorders. Hemophilia 2012; 18 Suppl 4:154-160.

Shattil SJ, Newman PJ. 2004. Integrins: dynamic scaffolds for adhesion and signalling in platelets. Blood 104:1606-1615.

Tadokoro S, Tomiyama Y, Honda S, Kashiwagi H, Kosugi S, Shiraga M, Kiyoi T, Kurata Y, Matsuzawa Y. 2002. Missense mutations in the β3 subunit have a different impact on the expression and function between αIIbβ3 and αvβ3. Blood 99:931-938.

Vinciguerra C, Khelif A, Alemany M, Morle F, Grenier C, Uzan G, Gulino D, Dechavanne M, Negrier C. 1996. A nonsense mutation in the GPIIb heavy chain (Ser870->stop) impairs platelet GPIIb-IIIa expression. Br J Haematol 95:399-407.

Ward CM, Kestin AS, Newman PJ. 2000. A Leu262Pro mutation in the integrin β3 subunit results in an αIIbβ3 complex that binds fibrin but not fibrinogen. Blood 96:161-169.

Watkins NA, Schaffner-Reckinger E, Allen DL, Howkins GJ, Brons NHC, Smith GA, Metcalfe P, Murphy MF, Kieffer N, Ouwehand WH. 2002. HPA-1a phenotype-genotype discrepancy reveals a naturally occurring Arg93Gln substitution in the platelet β3 integrin that disrupts the HPA-1a epitope. Blood 99:1833-1839.

Wilhide CC, Jin Y, Guo Q, Li L, Li SX, Rubin E, Bray PF. 1997. The human integrin beta3 gene is 63 kb and contains a 5'-UTR sequence regulating expression. Blood 90:3951-3961.

Xiao T, Takagi J, Coller BS, Wang J-H, Springer TA. 2004. Structural basis for allostery in integrins and binding to fibrinogen-mimetic therapeutics. Nature 432:59-67.

Yang J, Ma Y-Q, Page RC, Misra S, Plow EF, Qin J. 2009. Structure of an integrin αIIbβ3 transmembrane-cytoplasmic heterocomplex provides insight into integrin activation. Proc Natl Acad Sci USA 106:17729-17734.

Zhu J, Zhu J, Springer TA. 2013. Complete integrin headpiece opening in eight steps. J Cell Biol 201:1053-1068.

Figure 1. Mutation spectrum for *ITGA2B* and *ITGB3* in 76 GT families. Schematic representation of (I) *ITGA2B* cDNA and αIIb domain structure, in comparison with (II) *ITGB3* cDNA and β3 domain structure. In parts a), nucleotide variants are designated a symbol according to their type and grouped to the nearest exon. In parts b), missense mutations are identified by a single letter amino acid code. They are assigned to the structural domains of each subunit. Asterisks indicate the number of times the variant was found in apparently unrelated families in our study. In red are two missense mutations in *ITGA2B* predicted for exonic variants that also influence splicing and a single mutation in *ITGB3* affecting the signal peptide. cDNA accession numbers for *ITGA2B* and *ITGB3* are NM_000419.3 and NM_000212.2 respectively. UniProt accession numbers for αIIb and β3 are P08514 and P05106 respectively. Amino acid numbering is according to HGVS nomenclature with +1 corresponding to the translation initiating methionine. Mutations giving rise to GT are widely distributed across both genes.

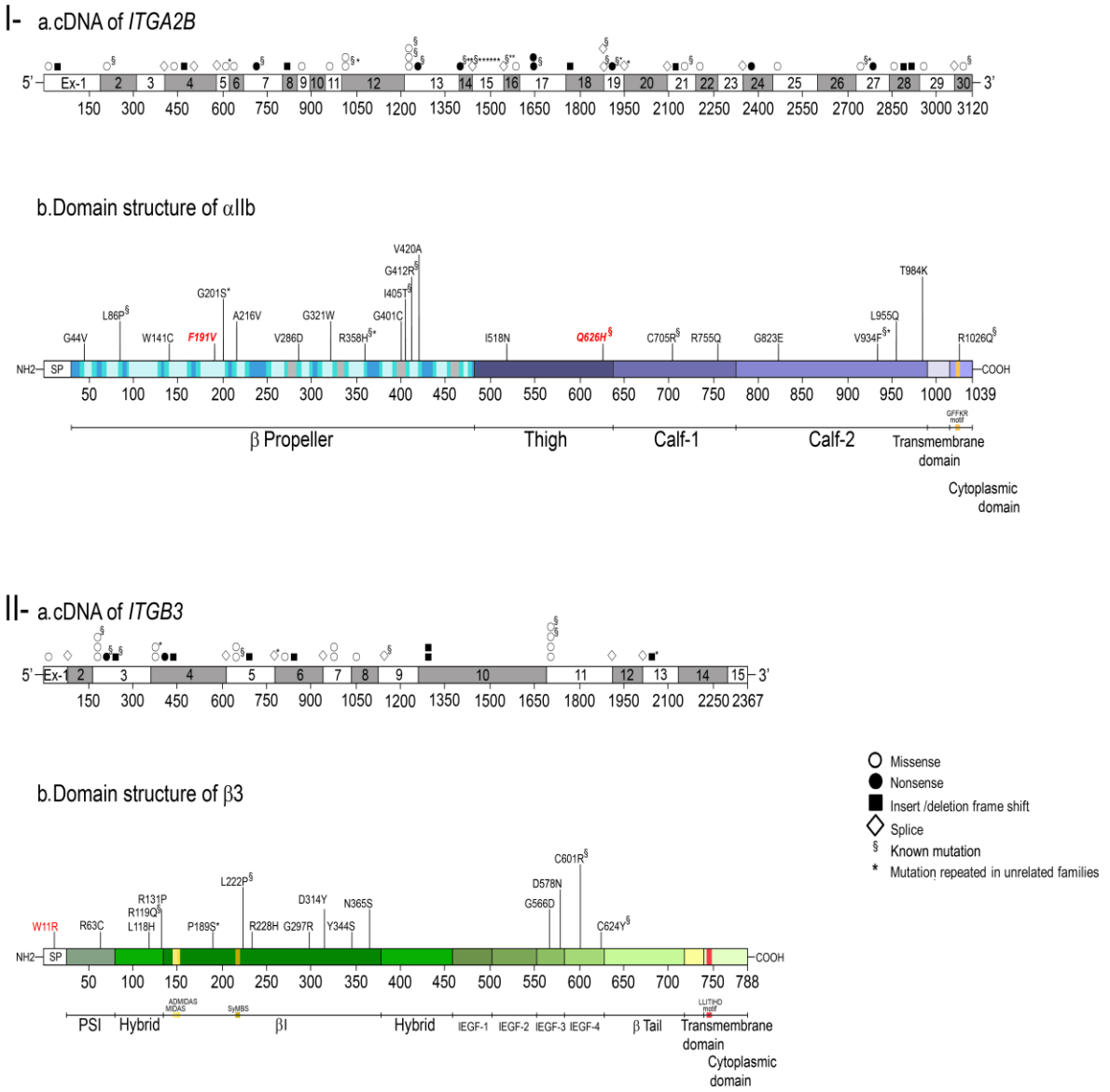

Figure 1.

Figure 2. Ribbon diagrams highlighting selected novel missense mutations within the αIIb β-propeller. The upper central panel shows the surface (front) of the propeller in contact with the βI domain of β3 and in the lower central panel we show the opposing side (back) of the propeller; red open circles localize the substituted amino acids that are identified in single letter code. Blade β-sheets are in pale blue, the FG-GAP motif in light green and Ca^{2+}-binding motifs in dark red. On the left side are enlarged views of the FG-GAP and Ca^{2+}-binding motifs with structuring H-bonds (dotted lines). Changes induced by p.Gly44Val, p.Gly201Ser, p.Ala216Val and p.Gly321Trp substitutions affecting FG-GAP motifs are shown in the upper windows. Val44 provokes steric encumbrance (red discs) predicted to break structuring H-bonds within the FG-GAP motif. Similar changes are predicted for p.Gly201Ser, p.Ala216Val and p.Gly321Trp. For the p.Val286Asp substitution (center panel) at the hydrophobic interior of the helix (blade 4), the introduced polar amino acid pushes apart the blades with entry of water molecules (blue spheres) that disrupt H-bonds and cause a major disturbance of β-propeller structure. Gly401 lies close to a calcium-binding motif given by 4 Asp residues within the third Ca^{2+}-binding loop on the far side of the β-propeller (the calcium atom is shown as a gray sphere). Structural changes include a loss of H-bonds extending from the substituted Gly. Mutations are illustrated as graphical sticks, amino acid residues engaged in H-bonds are represented as sticks with C atoms in white, N atoms in blue, O atoms in red and S atoms in orange. Models were obtained using the PyMol Molecular Graphics System, version 1.3 and the 3 fcs pdb file.

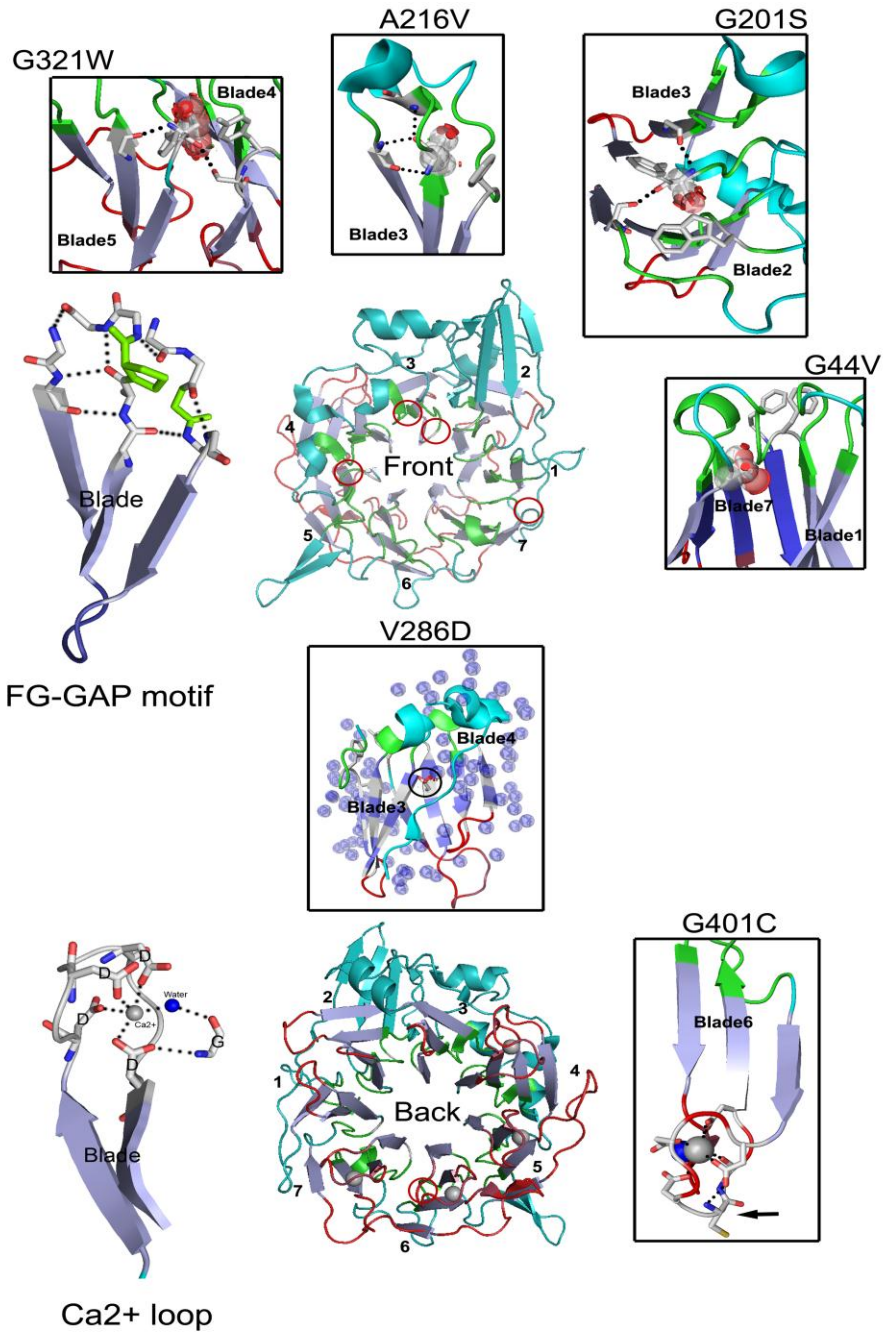

Figure 2.

Figure 3. Molecular representations of novel missense mutations within the αIIb calf-2 domain. Central is a ribbon diagram depicting the αIIb arm with the thigh domain in slate blue, the calf-1 domain in blue and the calf-2 domain in dark blue. The p.Gly823Glu, p.Thr984Lys and p.Leu955Gln substitutions are shown as red open circles; inserts show graphical representations of mutations with C atoms in white, N atoms in blue, O atoms in red and S atoms in orange; graphical "bumps" (red discs) reveal steric encumbrance caused by the amino acid substitution. Amino acids engaged in hydrogen (H)-bonds (dotted lines) are shown as sticks. Specifically, Glu823 pushes away the connecting ribbon between calf-1 and calf-2 resulting in an increased distance between Glu823 and Glu776, thereby opening the angle formed by calf-1 and calf-2 domains (left hand side windows). On the right hand side, windows illustrate the β-barrel structure of the calf-2 domain composed of 9 anti-parallel β-sheets. p.Leu995Gln and p.Thr984Lys substitutions result in the loss of a motif composed of five polar amino acids (Tyr784, His782, Ser754, Ser926 and Thr953) sharing H-bonds (dotted lines) within a largely hydrophobic region. Angle and distance measurements are indicated on the Figure. Hydrophobic lateral side-chains of β-sheet residues pointing inside the β-barrel structure of the calf-2 domain are in white. Models were obtained using the PyMol Molecular Graphics System, version 1.3 and the 3 fcs pdb file.

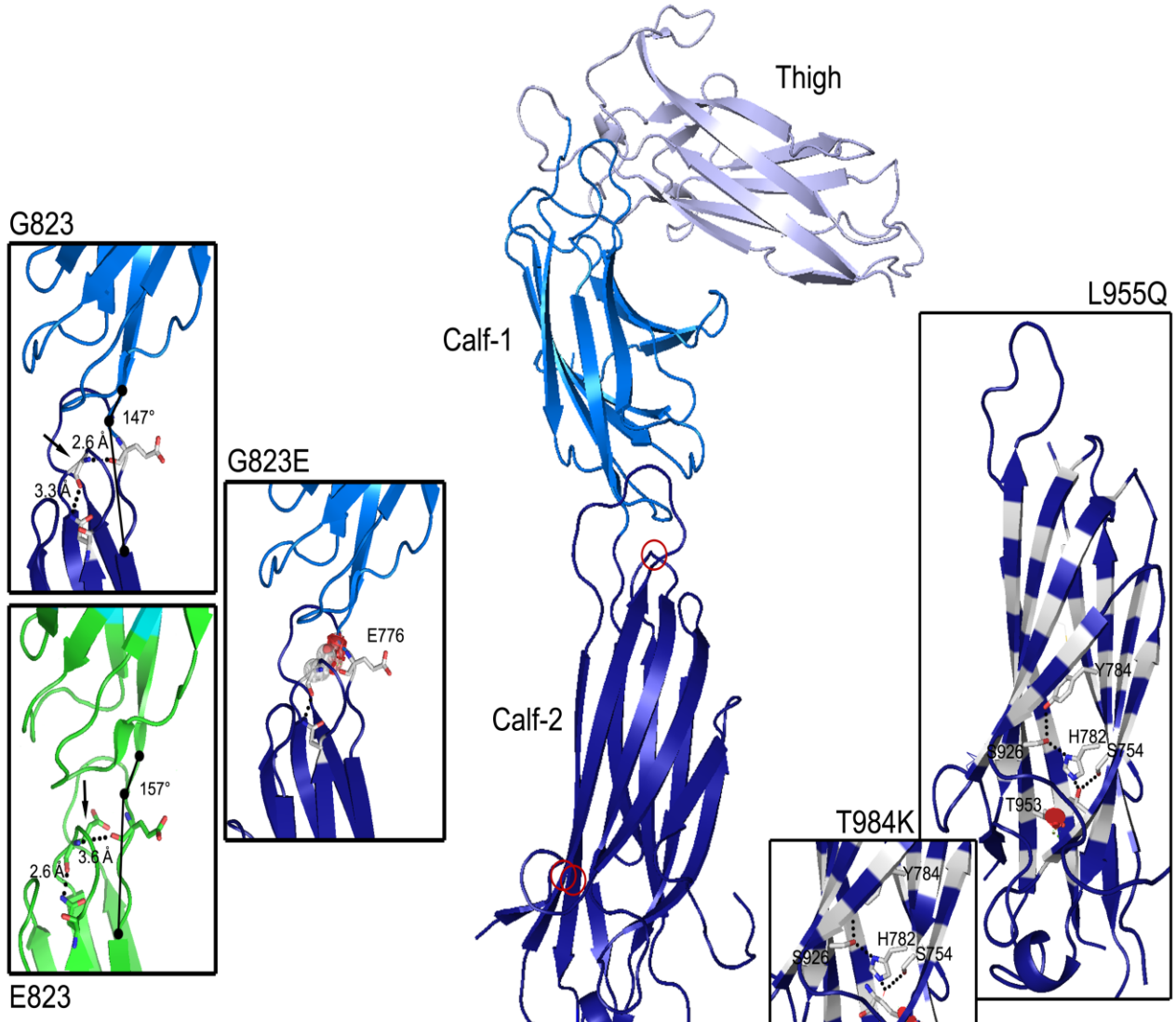

Figure 3.

Figure 4. Minigene studies of mRNA splicing following transient expression of selected constructs in COS-7 cells. Illustrated are the results for genomic sequencing, agarose gel electrophoresis of the amplified minigene cDNA PCR products, and direct PCR cDNA fragment sequencing. A/ A heterozygous T to G change at c.571 in exon4 and close to its boundary with intron 4 of *ITGA2B* for GT57 gave rise to similarly migrating PCR products when wild type and mutant minigene constructs were transfected in COS-7 cells with a 4 bp deletion revealed on sequencing. B/ The heterozygous intron 14 c.1440-13_c.1440-1del found in the *ITGA2B* gene of 7 unrelated type I GT patients also gave normally migrating minigene PCR products. However, direct sequencing shows a 2 bp deletion and activation of an upstream cryptic splice site in exon 15 C/ A homozygous c.2348+5G>C transversion in intron 23 of a type II patient (GT8) gave rise to a smaller and faster migrating minigene PCR product; direct sequencing of the major transcript confirmed skipping of exon 23.

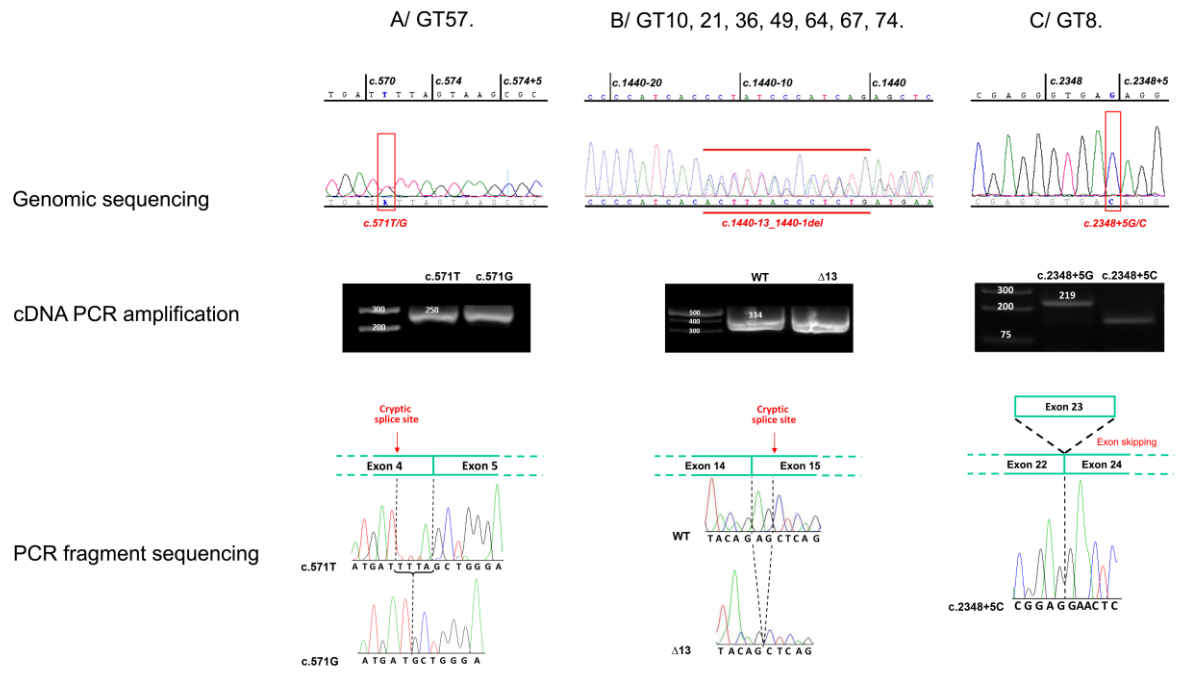

Figure 4.

Figure 5. Structural changes induced by selected missense mutations within the β3 extracellular domain. A ribbon diagram is shown in the center with the PSI domain in light green, the hybrid domain in green, the βI domain in dark green and the EGF-1 domain in green; red open circles situate the illustrated mutations. Residues of the active site SyMBS domain are represented as yellow sticks, those of the MIDAS domain in olive sticks and those of the adMIDAS domain as brown sticks. Ca^{2+} and Mg^{2+} atoms are shown as gray and pale blue spheres respectively. The p.Arg63Cys mutation (right lower panel) in the PSI domain is close to disulfides within the PSI or connecting PSI and EGF-1 domains. The introduced Cys63 is available to competitively interact with Cys52 or other nearby Cys residues, the result is pro-αIIbβ3 complex formation but a block in maturation (see Supp. Fig. S4). Both p.Arg131Pro and p.Leu118His are novel mutations within the hybrid domain. The p.Arg131Pro change results in a β-turn in the connecting ribbon with the upper βI domain. In contrast, p.Leu118His directly involves the β-barrel structure of the hybrid domain (hydrophobic residues pointing to the interior are in white); it introduces a larger polar amino acid into the hydrophobic region with steric encumbrance. Both p.Asp314Tyr and p.Pro189Ser affect β3Arg287 (shown as dark green spheres in the insets), a β3 residue penetrating deep within the αIIb β-propeller. The p.Asp314Tyr substitution results in steric encumbrance that pushes away the small 3-10 helix bearing Arg287. The p.Gly297Arg substitution introduces steric encumbrance at the interface between αIIb and β3 headpieces. Tyr344 lies close to the metal coordination sites of the βI domain; its replacement by the smaller Ser results in loss of a structuring H-bond (dotted line) with Ala252 beside Asp251 of the MIDAS site. C atoms are colored in white, N atoms in blue, O atoms in red and S atoms in orange. Graphical “bumps” (red discs) indicate steric encumbrance. Amino acid residues engaged in H-bonds are shown as sticks. Disulfides are represented as lines. In the case of the p.Arg63Cys substitution, distance measurements separating Cys residues are indicated on the

figure. Models were obtained using the PyMol Molecular Graphics System, version 1.3 and the 3 fcs pdb file.

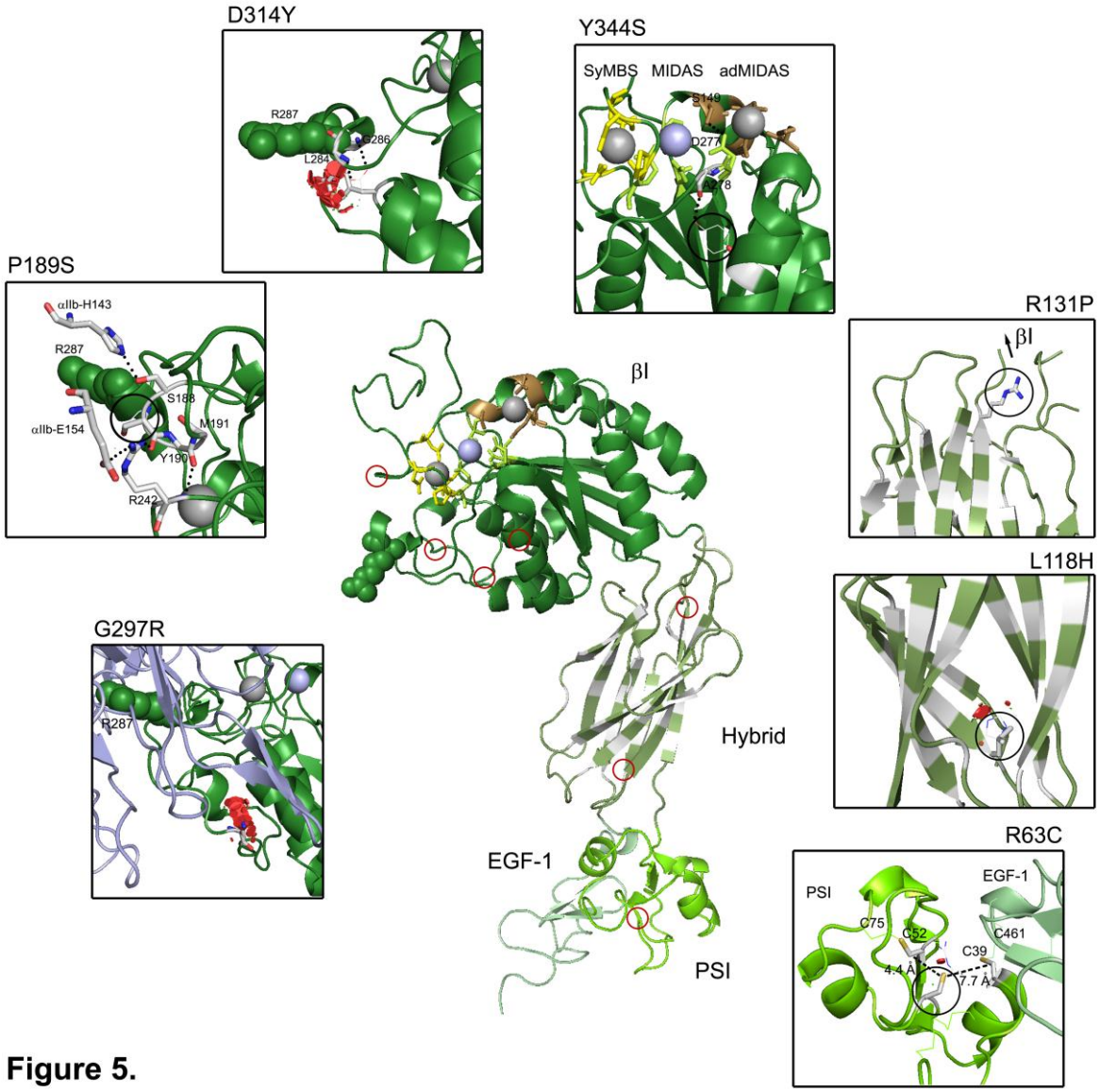

Figure 5.

Table 1. Phenotype/Genotype correlations with respect to bleeding score

	Total				Genotyped				Type I			Type I		
	I (n)	II (n)	var (n)	p	I (n)	II (n)	var (n)	p	ITGA2B (n)	ITGB3 (n)	p	missense (n)	other (n)	p
WHO Bleeding score														
1	1	3	2	0.02*	1	2	1	0.022*	0	1	0.211	1	0	0.445
2	17	2	1		16	2	0		12	4		9	7	
3	26	2	3		21	2	0		10	11		10	11	
4	19	2	2		18	2	0		11	7		6	12	

Total: All enrolled cases for whom clinical data was available.
Genotyped: Patients with homozygous or composite heterozygous mutations in ITGA2B or ITGB3 genes.
Type I: GT type I patients with homozygous or composite heterozygous mutations in ITGA2B or ITGB3 genes.
*denotes statistical two sided Fisher's Exact Test significance.

Appendix: The authors also acknowledge the role of the following additional participants in patient recruitment and collecting data

Dr. Ismaïl El Alamy, Laboratoire d'Explorations Fonctionnelles Plaquettaires, Hôpital Tenon, Paris, France; *Dr. Marie-Elizabethe Briquel*, Service d'Hématologie-Biologique, Hôpital de Brabois, CHU de Nancy, Vandoeuvre-les-Nancy, France; Professor Hervé Chambost, Service de Pédiatrie et Hématologie Pédiatrique, Hôpital de la Timone, Marseille, France; Dr. Ségolène Claeyssens, Service de Pédiatrie – Hématologie, Oncologie, CHU de Toulouse, Toulouse, France; *Dr. Bénédicte Delahousse*, Service d'Hématologie-Hémostase, Hôpital Trousseau, Tours, France; *Professeur Ginès Escolar*, Hospital Clinic, Servicio de Hemoterapia y Hemostasia, Barcelona, Spain; *Dr. Remi Favier,* Service d'Hématologie Clinique, Hôpital d'Enfants Armand-Trousseau, Paris, France; Dr. Michel Laguerre, Institut Européen de Chimie et Biologie, Pessac, France; *Professor Thomas Lecompte*, Hemostasis Unit and Haematology Department, University Hospital of Geneva, Geneva, Switzerland; *Dr. Desiree Medeiros*, Kapiolani Medical Center for Women and Children, Honolulu, Hawaii, USA; *Dr. Maguy Micheau,* Service d'Hématologie Biologique, Hôpital Pellegrin, CHU Bordeaux, Bordeaux, France; *Professor Philippe Moerloose*, Haemostasis Unit, Geneva University Hospitals, Geneva, Switzeland; *Professor Marta Pico*, Servicia Hemostasia, Hospital Val d'Hebron, Barcelona, Spain; *Dr. Catherine Pouymayou*, Laboratoire d'Hématologie, Hôpital La Timone, Marseille, France; *Dr. Markus Schmugge*, Division of Haematology, University Childrens Hospital, Zürich, Switzerland; *Dr. David Wilcox*, Blood Research Institute, Blood Center of Wisconsin, Milwaukee, Wisconsin, USA.

